Hindawi
Advances in Civil Engineering
Volume 2019, Article ID 1432697, 11 pages
https://doi.org/10.1155/2019/1432697

Research Article

Torsional Behavior of High-Strength Concrete Beams with Minimum Reinforcement Ratio

Changbin Joh,[1] **Imjong Kwahk**,[2] **Jungwoo Lee**,[2] **In-Hwan Yang**,[3] **and Byung-Suk Kim**[4]

[1]*Research Fellow, Korea Institute of Civil Engineering and Building Technology, Department of Infrastructure Safety Research, Goyang, Gyeonggi 10223, Republic of Korea*
[2]*Senior Researcher, Korea Institute of Civil Engineering and Building Technology, Department of Infrastructure Safety Research, Goyang, Gyeonggi 10223, Republic of Korea*
[3]*Professor, Kunsan National University, Department of Civil Engineering, Kunsan, Jeonbuk 54150, Republic of Korea*
[4]*Senior Research Fellow, Korea Institute of Civil Engineering and Building Technology, Department of Infrastructure Safety Research, Goyang, Gyeonggi 10223, Republic of Korea*

Correspondence should be addressed to Changbin Joh; cjoh@kict.re.kr

Received 25 April 2018; Revised 18 September 2018; Accepted 18 October 2018; Published 17 January 2019

Academic Editor: Constantin Chalioris

Although there is a growing trend to use higher strength for concrete and steel in reinforced concrete structures due to the lightness and slenderness of these members together with the simplified arrangement of their reinforcement, there is still the necessity to inspect the reduction of ductility resulting from the gain in strength. Taking into account that this also concerns the design for torsion, this study intends to investigate the regulations related to the torsional minimum reinforcement ratio in view of the minimum ductility requirement with focus on Eurocode 2. To that goal, the relation between the torsional cracking moment and the ductile behavior is discussed for the beam reinforced with the minimum torsional reinforcement ratio to examine the eventual properness of the minimum torsional reinforcement ratio recommended by Eurocode 2. Moreover, a pure torsion test is performed on 18 beams made of 80 MPa concrete reinforced by high-strength bars with rectangular section and various test variables involving the minimum torsional reinforcement ratio, the transverse-to-longitudinal reinforcement ratio, and the total reinforcement ratio. As a result, for the high-strength concrete beams, the minimum torsional reinforcement ratio recommended by Eurocode 2 was insufficient to prevent the sudden loss of strength after the initiation of the torsional cracking. But with regard to the compatibility torsion of statically indeterminate structure, the adoption of the minimum torsional reinforcement ratio recommended by Eurocode 2 might secure enough deformability under displacement-controlled mode to allow the redistribution of the torsional moment.

1. Introduction

There is a growing trend to use higher strength for concrete and steel in reinforced concrete structures. The near future will see wider application of members applying concrete with the compressive strength higher than 80 MPa and reinforced by steel with the yield strength of 600 MPa. This new popularity is due to the lightness and slenderness of these members together with the simplified arrangement of their reinforcement. However, there is still the necessity to inspect the reduction of ductility resulting from the gain in strength. Need is thus to verify if the current design codes under force are capable to control adequately the strength-ductility balance. Particularly, the regulations related to the minimum reinforcement ratio should be examined in view of the minimum ductility requirement.

This also concerns the design for torsion. In general, similar to the minimum reinforcement for shear and flexure, the minimum torsional reinforcement intends to provide the member with sufficient postcracking torsional resistance.

This means controlling the crack width and securing enough ductility to prevent sudden loss of the torsional strength after cracking. Numerous researchers, however, already pointed out the issues resulting from the behavioral change brought by the increase of the strength or related to the minimum torsional reinforcement ratio recommended by ACI 318-14 Code or Eurocode 2 (EC 2) [1–19].

Rasmussen and Baker [3] and Lopes and Bernardo [4] compared the torsional characteristics of reinforced beams made of normal concrete and high-strength concrete and concluded that the use of high-strength concrete was favorable with respect to the torsional stiffness and the stress in the reinforcement but increased the brittle tendency after cracking. Chiu et al. [5] performed pure torsion tests on beams made of normal concrete and high-strength concrete to investigate the effect of the minimum reinforcement ratio in the longitudinal and transverse directions. Based upon their experimental results, these authors reported that the postcracking strength, i.e., the ductile failure mode, depended significantly on the total reinforcement ratio in the longitudinal and transverse directions as well as the ratio of the longitudinal to the transverse reinforcement. This dependency was more marked in the high-strength concrete members than in those made of normal concrete. Ismail [6], who performed a literature review on previous torsion tests, and Yoon et al. [7], who studied experimentally the effect of high-strength reinforcement, also reported that the use of high-strength concrete favored the occurrence of the brittle behavior beyond the torsional strength.

Numerical methods were also studied. Rahal and Collins [8, 9] successfully applied the modified compression field theory to estimate the torsional behavior of concrete beams, and Chalioris [10] combined the smeared crack model and the softened truss model to predict the initial torsional stiffness, torsional cracking moment, and strength of concrete beams. Bernardo and Lopes [11] proposed a parameter for the plastic behavior and twist capacity of high-strength concrete hollow beams based on the analysis of their test.

In concern with the minimum torsional reinforcement ratio, Koutchoukali and Belarbi [12] stated that the minimum torsional reinforcement of ACI 318-95 Code [13] was inadequate for high-strength concrete beams and stressed the necessity to provide at least 20% reserve of strength after cracking to prevent the brittle failure. Both Ali and White [14] and Kim et al. [15] indicated the problems of the minimum torsional reinforcement ratio and proposed new minimum reinforcement ratios enabling to maintain the postcracking strength.

Accordingly, this study intends to investigate the appropriateness of the current design codes for torsion with focus on EC 2. To that goal, the relation between the minimum torsional reinforcement ratio and the torsional cracking moment is analyzed theoretically, and the pure torsion test is performed on beams made of 80 MPa concrete reinforced by high-strength reinforcement. Moreover, the relation between the torsional cracking moment and the ductile behavior is discussed for the beam reinforced with the minimum torsional reinforcement ratio to examine the eventual properness of the minimum torsional reinforcement ratio recommended by EC 2.

2. Minimum Torsional Reinforcement Ratio and Torsional Cracking Moment

Since the torsional design methods of EC 2 and ACI 318-14 Code provide conceptually identical minimum torsional reinforcement, this study analyzes theoretically the relation between the minimum torsional reinforcement and the torsional cracking moment (T_{cr}) with reference to EC 2.

In EC 2, the torsional load is decomposed into shear forces applied in each face of the member, and design is performed only with respect to these shear forces. Therefore, $\rho_{v,min}$ can be expressed as follows in function of the tensile strength of concrete and the yield strength of the stirrups:

$$\rho_{v,min} = \frac{A_{v,min}}{sb_w} = 0.08\frac{\sqrt{f_{ck}}}{f_{yv}}, \quad (1)$$

where $A_{v,min}$ = cross-sectional area of minimum shear reinforcement; s = spacing of stirrups; b_w = width of the cross section; f_{ck} = compressive strength of concrete; and f_{yv} = yield strength of shear and torsional reinforcement.

Besides, according to the theory of the thin-walled tube and the space truss analogy, the torsional cracking strength (T_{cr}) and the torsional strength (T_n) can be expressed as follows [1, 20]:

$$T_{cr} = 2A_0 t f_t, \quad (2)$$

$$T_n = \frac{2A_0 A_t f_{yv}}{s}\cot\theta, \quad (3)$$

where t = effective thickness of the tube resisting to torsion; A_0 = internal area inside the central axis of effective thickness; f_t = tensile strength of concrete; A_t = cross-sectional area of closed torsional stirrup; and θ = angle of crack.

In Equation (2), the tensile strength of concrete can be assumed as $f_t = 0.33\sqrt{f_{ck}}$ [1, 20]. The beam in torsion can be seen to be in a biaxial state under the simultaneous occurrence of compression and tension, and accordingly, the concrete tensile strength can be lowered compared to the uniaxial tension state. Following, Equation (2) can be rewritten as

$$T_{cr} = 2A_0 t\left(0.33\sqrt{f_{ck}}\right). \quad (4)$$

Besides, if $\rho_{v,min}$ is accepted in the usual way as the minimum reinforcement ratio enabling the member to maintain ductility without sudden loss of the torsional strength after cracking, $T_{cr} = T_n$ and the following equation is obtained by equaling Equations (3) and (4):

$$T_{cr} = 2A_0 t\left(0.33\sqrt{f_{ck}}\right) = \frac{A_t f_{yv}}{s}\left(2A_0\right)\cot\theta. \quad (5)$$

If the beam is not prestressed and is reinforced equally in the transverse and longitudinal directions, the crack angle θ

can be assumed to be 45°. Consequently, Equation (5) can be rewritten as follows:

$$\frac{A_t f_{yv}}{st} = 0.33\sqrt{f_{ck}}. \quad (6)$$

According to EC 2 (EN 1992-1-1:2004 6.3.2 (1)), the effective thickness, t, may be taken as the total cross-sectional area ($A_{cp} = b_w h$, h = height of the section) divided by the outer circumference of the cross section ($p_{cp} = 2(b_w + h)$). To make the discussion as simple and practical as possible, only rectangular members are considered here. Considering the aspect ratio of the cross section $h/b_w = 1 \sim 10$, t ranges between $0.25b_w$ and $0.45b_w$. Accordingly, the reinforcement ratio resisting to T_{cr} can be obtained by the following equation:

$$\rho_v = \frac{A_v}{sb_w} = \frac{2A_t}{sb_w} = (0.165 \sim 0.297)\frac{\sqrt{f_{ck}}}{f_{yv}}. \quad (7)$$

This value corresponds to about 2 to 3.7 times the minimum reinforcement ratio given in Equation (1) as suggested by EC 2.

From Equation (7), $\rho_v f_{yv}$ can be expressed as a function of f_{ck}. This function is plotted in Figure 1 together with the values recommended by EC 2, ACI 318-14, CSA-04, MC2010, and KCI by applying the condition $T_{cr} = T_n$ [21–24].

It appears that the minimum reinforcement ratio $\rho_{v,min}$ must be 2 to 3.7 times the value required by EC 2 to satisfy the condition $T_{cr} = T_n$. This indicates that the application of the current $\rho_{v,min}$ recommended by the design codes presents high risk of strength loss to occur after the initiation of torsional cracking.

3. Torsion Test

3.1. Material Characteristics. The concrete used in the fabrication of the torsional members is a high-strength concrete developing 80 MPa class compressive strength. Table 1 arranges the mix composition for 1 m^3. In Table 1, S/a and SP/B stand, respectively, for sand-to-aggregate ratio and superplasticizer-to-binder ratio; OPC, BS, and FA designate, respectively, ordinary Portland cement, blast furnace slag, and fly ash.

Six batches of concrete with the same mix composition were used to fabricate 6 series of specimens. The specimens were subjected to air-dry curing during 24 hours followed by 24 hours of high-temperature steam curing at 90°C. The same curing process was applied to the cylinders used to measure the compressive strength and the splitting tensile strength (Figure 2).

The average compressive strength of each batch is arranged in Table 2. The average of the elastic modulus measured on 19 cylinders is 41.6 GPa. The average of the splitting tensile strength measured on 28 cylinders is 3.7 MPa.

Table 3 lists the measured yield strength of the reinforcement used in the fabrication of the specimens. These values were reflected in the design of the specimens.

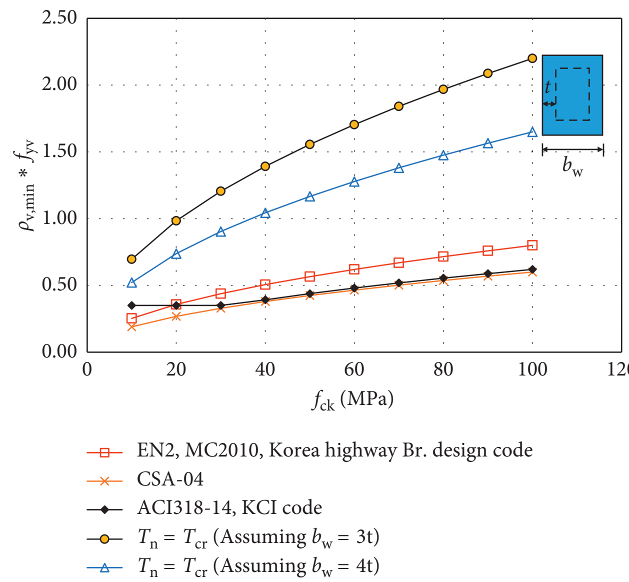

Figure 1: Minimum reinforcement ratio and torsional cracking moment.

Even if it is better to use rebar-like D6 (A_s = 31.63 mm^2) with the smallest area as possible to adjust precisely the reinforcement ratio of the specimens, there was no availability of bars smaller than D10 in the market and the bars listed in Table 3 were used to fabricate the specimens. Moreover, the SD600 D10 bar is not available in the market and there was difficulty to secure SD500 D19 bar nor SD600 D13 and D19.

3.2. Test Variables and Details of Specimens. Table 4 arranges the designation and characteristics of the 18 beam members that were designed and fabricated in this study. These specimens were planned to evaluate the effect of the minimum torsional reinforcement ratio ($\rho_{v,min}$) specified by EC 2, transverse-to-longitudinal reinforcement ratio ($\rho_t f_{yv}/\rho_l f_{yl}$), total reinforcement ratio (ρ_{t+l}), and yield strength of the reinforcement (f_{yv}, f_{yl}) on the torsional behavior. Here, ρ_t, ρ_l, and ρ_{t+l} are the volumetric ratios.

All the high-strength concrete specimens present the same rectangular cross section of 300 × 400 mm for a total length of 3 m. Figure 2 shows representative cross section and reinforcement details. The clear concrete cover is 30 mm, and 135° hook is used for all stirrups.

The designation of the specimens includes 5 fields specifying their characteristics. The first field RA means rectangular section A to prepare for future tests on members with other cross sections. The second section (SD4, SD5, and SD6) indicates the steel grade of the adopted reinforcement (SD400, SD500, and SD600). The third field indicates the ratio of the stirrup ($\rho_v = 2A_t/(b_w s)$) to $\rho_{v,min}$ of EC 2. The fourth field corresponds to the transverse-to-longitudinal reinforcement ratio ($\rho_t f_{yv}/\rho_l f_{yl}$). The fifth field represents the total reinforcement ratio (ρ_{t+l}).

The 18 specimens are classified into 6 series of 3 specimens reinforced with different steel grades (SD400, SD500,

Table 1: Mix composition for 1 m^3 of high-strength concrete.

W/B (%)	W (kg)	S/a (%)	SP/B (%)	Mixture (kg)						
				OPC	BS	FA	Sand (sea)	Sand (crushed)	Aggregate 19 mm	SP
0.24	164	0.45	1.30	420.0	224.0	56.0	403.3	271.0	827.9	9.101

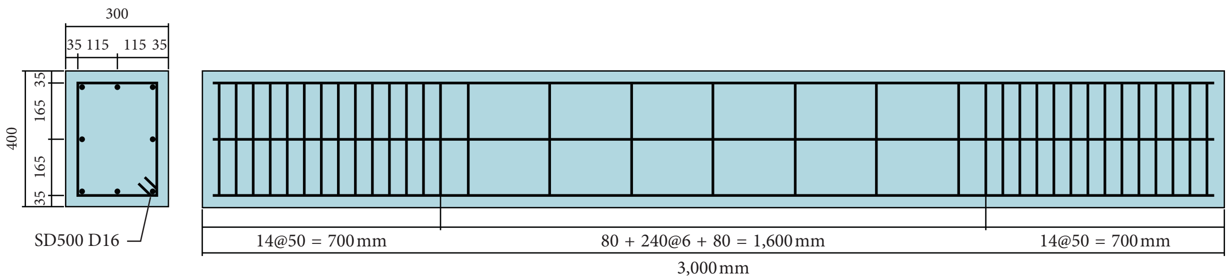

Figure 2: Typical reinforcement details of the specimen (RA-SD5-1.5-0.2-1.62).

Table 2: Compressive strength and splitting tensile strength of high-strength concrete.

Number of the batch	Average compressive strength		Average splitting tensile strength	
	Strength (MPa)	Number of cylinders	Strength (MPa)	Number of cylinders
1	80.0	4	3.5	3
2	72.8	4	3.8	5
3	73.7	5	3.2	5
4	84.7	5	3.7	5
5	83.1	5	3.9	5
6	90.0	5	4.0	5

Table 3: Nominal area and yield strength of steel reinforcement.

Reinforcement		D10	D13	D16	D19	D22
Nominal area, A_s (mm^2)		71.33	126.7	198.6	286.5	387.1
Yield strength, f_y (MPa)	SD400	483.8	474.1	394.6	456.1	452.3
	SD500	538.0	522.4	529.0	N/A	499.4
	SD600	N/A	N/A	627.0	N/A	630.9

and SD600). Apart from the steel grade, each series gathers 3 similar test variables. All the specimens are reinforced transversally by D10 stirrups. Note that the third specimen in each series uses SD500 D10 instead of the nonavailable SD600 D10 and that SD600 is used only for the longitudinal reinforcement.

Figure 3 shows how the specimens were designed with respect to minimum reinforcement ratios. Series 1 and 2 involve the specimens designed to approach at the most $\rho_{v,min}$ of EC 2 by applying D10 stirrups in order to examine the behavior of the torsional members with the minimum torsional reinforcement. Since D10 stirrups are used in Series 1, the spacing s of the stirrups was increased from the minimum of 175 mm prescribed by EC 2 to 240 mm to lower as possible ρ_t. The design also adopted values between 0.2 and 0.3 for $\rho_t f_{yv}/\rho_l f_{yl}$ and 1.62% for ρ_{t+l} to exceed the minimum of 1% required by ACI 318-14. Similarly to Series 1, the reinforcement of Series 2 was arranged to be as close as possible to achieve the minimum reinforcement ratio. The difference is that $\rho_t f_{yv}/\rho_l f_{yl}$ was increased to let ρ_{t+l} be smaller than 1% with a value of 0.92%. This means that the members of Series 2 have the smallest amount of reinforcement.

Series 3, 4, and 5 all with $\rho_t = 3.2 \times \rho_{v,min}$ are intended to evaluate the effect of ρ_{t+l} and $\rho_t f_{yv}/\rho_l f_{yl}$ on the torsional behavior. The specimens of Series 3 were reinforced with $\rho_t f_{yv}/\rho_l f_{yl}$ of Series 1. Series 4 presents ρ_t similar to Series 3 but with increased $\rho_t f_{yv}/\rho_l f_{yl}$ to lower ρ_{t+l} to the level of Series 1 within a range of 1.63% to 2.13%. Series 5 is reinforced as Series 3 but with further increase of $\rho_t f_{yv}/\rho_l f_{yl}$ compared to Series 4 so that ρ_{t+l} approaches 1%.

Series 6 is intended for comparing the torsional behavior with that of Series 5. In Series 6, ρ_t is set to about 5 times $\rho_{v,min}$ and $\rho_t f_{yv}/\rho_l f_{yl}$ is increased to minimize ρ_{t+l} range between 2.00% and 2.49% so as to lower ρ_l.

3.3. Test Method. Figure 4 depicts the experimental setup for the pure torsion test. The torsional member was loaded vertically through steel beams disposed at its extremities to make the 1,600 mm long part at its center be in pure torsion. Each end support was hinged by two cylindrical blocks with lubricated surfaces (Figure 4), which allows not only rotation but also longitudinal motion. Loading was applied through displacement control at a speed of 1.0 mm/min (the duration of a test in average was 60 minutes). The rotation angle was calculated based upon the deflections measured by two displacement transducers (DT) disposed along the portion of the member in pure torsion.

Table 4: Designation and reinforcement details of specimens.

Series	Designation of specimen	Concrete strength	Reinforcement details							
			Stirrup				Longitudinal			
		f_{ck} MPa	A_t mm^2	f_{yv} MPa	Spacing mm	ρ_t %	A_l mm^2	f_{yl} MPa	Number of rebars	ρ_l %
	RA-SD4-1.3-0.3-1.62			484		0.293		395		1.324
1	RA-SD5-1.5-0.2-1.62	80.0		538		0.293	D16	529	8	1.324
	RA-SD6-1.5-0.2-1.62			538	240	0.293		627		1.324
	RA-SD4-1.3-0.5-0.92			484		0.289	D13	474	6	0.634
2	RA-SD5-1.5-0.5-0.92	72.8		538		0.289	D13	522	6	0.634
	RA-SD6-1.5-0.4-0.95			538		0.289	D16	627	4	0.662
	RA-SD4-3.2-0.3-3.28			484	100	0.695		452		2.581
3	RA-SD5-3.2-0.3-3.21	73.7		538	110	0.631	D22	499	8	2.581
	RA-SD6-3.2-0.2-3.21		D10	538	110	0.631		630		2.581
	RA-SD4-3.2-0.5-2.13			484	100	0.702	D19	456		1.433
4	RA-SD5-3.2-0.7-1.63	84.7		538	110	0.638	D16	529	6	0.993
	RA-SD6-3.2-0.6-1.63			538	110	0.638	D16	627		0.993
	RA-SD4-3.2-1.1-1.33			484	100	0.695	D13	474	6	0.634
5	RA-SD5-3.2-1.0-1.26	83.1		538	110	0.631	D13	522	6	0.634
	RA-SD6-3.2-0.8-1.26			538	110	0.631	D16	627	4	0.662
	RA-SD4-5.4-1.1-2.49			484	60	1.700		395	8	1.324
6	RA-SD5-5.1-1.0-2.00	90.0		538	70	1.003	D16	529	6	0.993
	RA-SD6-5.1-0.9-2.00			538	70	1.003		627	6	0.993

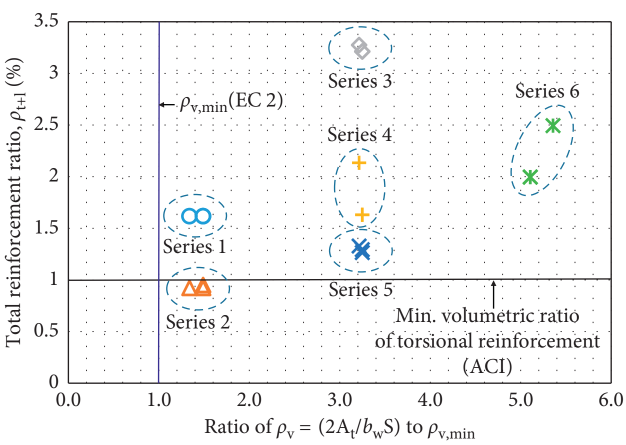

Figure 3: Reinforcement ratios of specimens and minimum reinforcement requirement.

For Series 1 and 2, the test was conducted up to the rotation that gives 50% of the peak (the maximum torsional moment) after the peak in order to examine the postcracking deformability of the beams. The other series were tested up to the rotation that gives 75% of the peak after the peak.

4. Test Results and Discussion

4.1. Cracking Pattern. Figure 5 illustrates the cracking patterns of the 6 series of specimens. In order to conduct objective comparison, the cracking patterns are shown for the specimens reinforced by SD400 reinforcement. Note that the patterns are similar for SD500 and SD600.

For Series 1 and 2 with ρ_t close to $\rho_{v,min}$ of EC 2 (Figures 5(a) and 5(b)), the torsional strength is seen to decrease after the initiation of the cracks. The specimens of both series did not show particular difference in their cracking behavior. After the first cracks, almost no additional cracks were developed and the initial cracks increased to failure. Consequently, as theoretically implied in Section 2, this indicates that $\rho_{v,min}$ of EC 2 cannot prevent brittle failure after cracking regardless of the satisfaction of $\rho_{t+l} \geq 1\%$.

For Series 3, 4, and 5 in which $\rho_t = 3.2 \times \rho_{v,min}$, the postcracking torsional strengths increased and additional cracks were developed with ductile behavior (Figures 5(c)–5(e)). It appears that relatively better distribution of the cracks occurred with larger ρ_{t+l}. Series 5 in Figure 5(e) exhibited ductile behavior owing to the relatively large value of $\rho_t = 3.2 \times \rho_{v,min}$ even if ρ_{t+l} (1.33%) was smaller than 1.62% of Series 1.

For Series 6 with the largest ρ_t in Figure 5(f), ρ_{t+l} (2.49%) was smaller than 3.28% of Series 3 (Figure 5(c)) but the cracks were distributed more evenly to develop the better ductile behavior at the end. It should be noted that the shorter spacing of stirrups (60 or 70 mm) compared to the other series increased the concrete confinement and influenced the torsional response [25].

4.2. Torsion-Displacement Behavior

4.2.1. Minimum Torsional Reinforcement Ratio ($\rho_{v,min}$) and Deformability. Figures 6(a) and 6(b) plot the relation between the torsion and the rotation angle for Series 1 and 2. The specimens of both series were reinforced by 1.3 to 1.5 times $\rho_{v,min}$ of EC 2 but could not resist to the torsional cracking moment (T_{cr}) after cracking. This brittle failure mode is expected in Section 2, and Koutchoukali and Belarbi [12] and Chiu et al. [5] also reported similar brittle behaviors in the specimens with

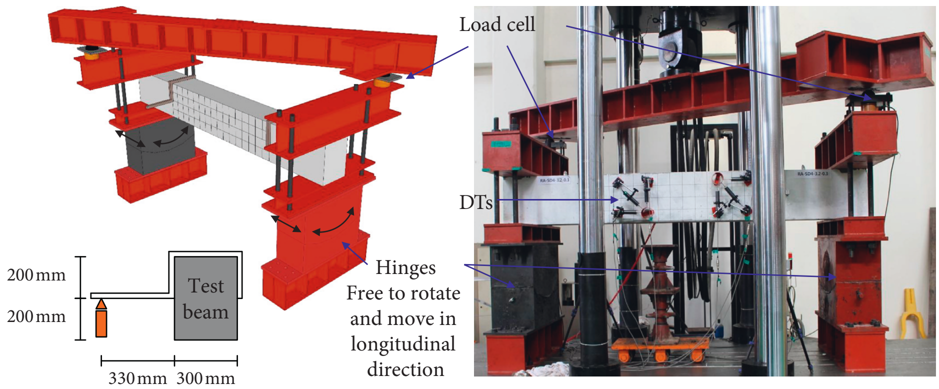

Figure 4: Setup of the torsion test.

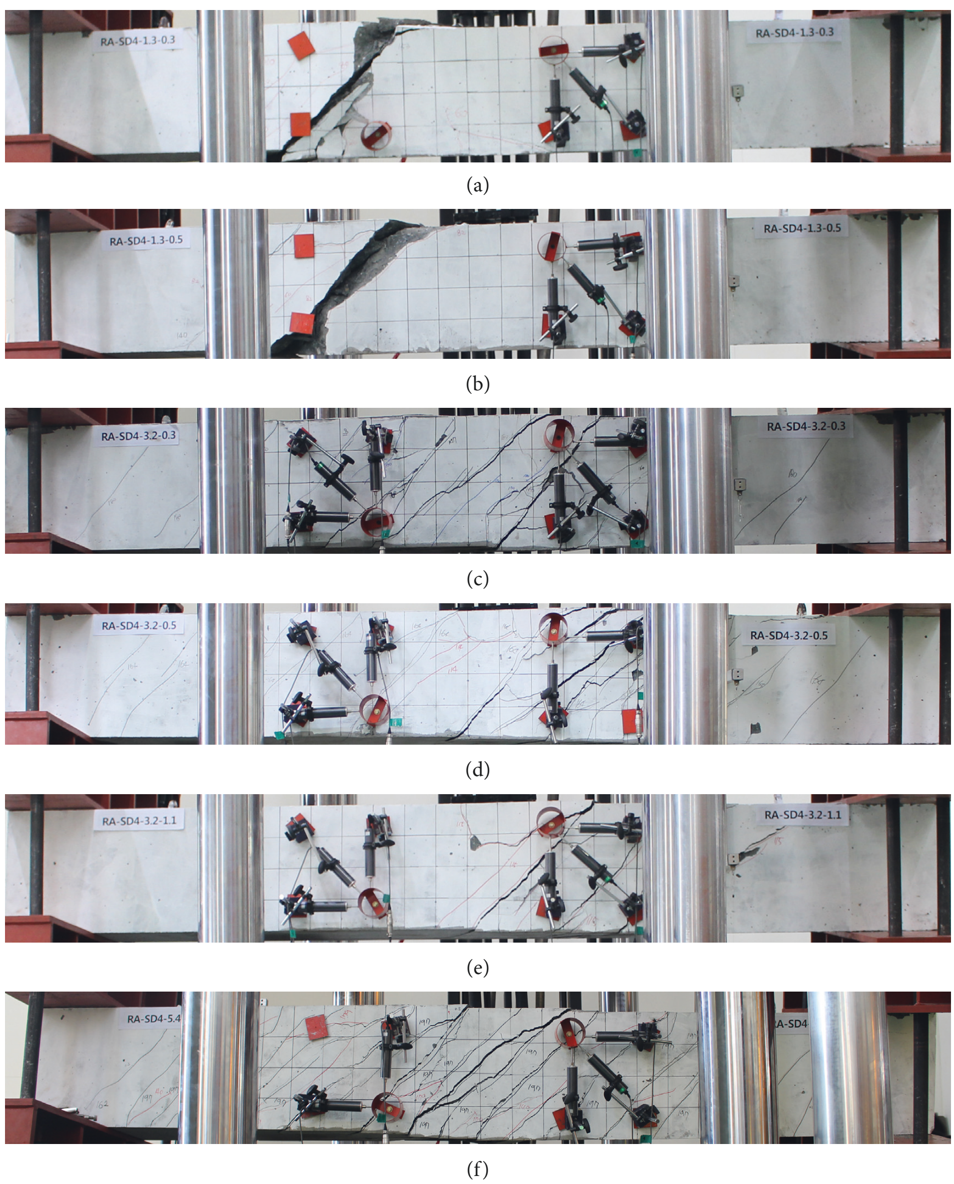

Figure 5: Cracking patterns of high-strength beams reinforced by SD400 bars. (a) Series 1: RA-SD4-1.3-0.3-1.62. (b) Series 2: RA-SD4-1.3-0.5-0.92. (c) Series 3: RA-SD4-3.2-0.3-3.28. (d) Series 4: RA-SD4-3.2-0.5-2.13. (e) Series 5: RA-SD4-3.2-1.1-1.33. (f) Series 6: RA-SD4-5.4-1.1-2.49.

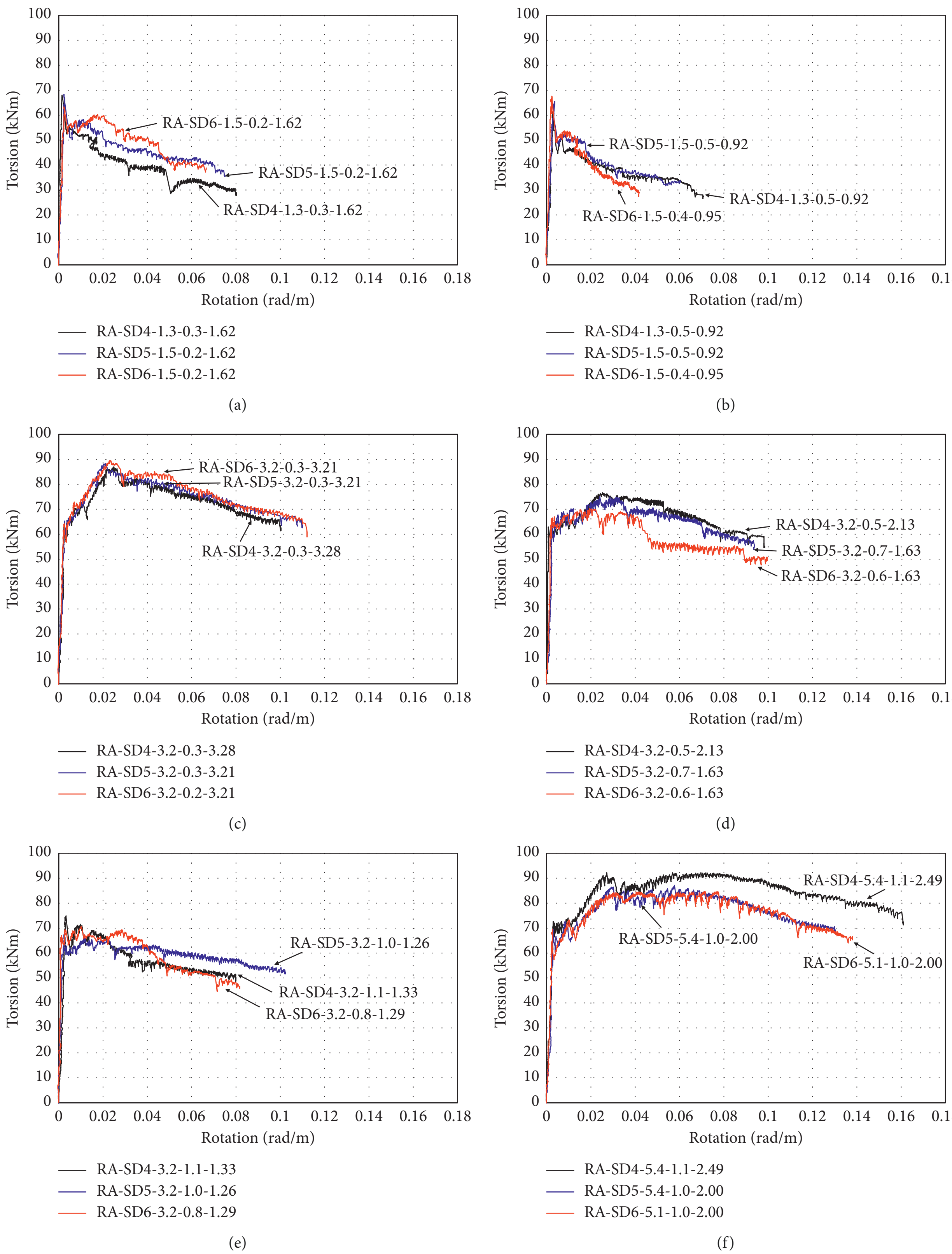

Figure 6: Torsional behavior of high-strength beams. (a) Series 1. (b) Series 2. (c) Series 3. (d) Series 4. (e) Series 5. (f) Series 6.

the reinforcement close to $\rho_{v,min}$. It seems that $\rho_{v,min}$ of EC 2 is not sufficient to maintain the torsional strength after cracking.

Nevertheless, all the specimens of Series 1 and 2 exhibited meaningful deformability in the test conducted through displacement control. Loss of the resistance to torsion occurred instantly at the initiation of cracking but the reinforcement took rapidly charge of the load and enabled the specimens to recover their resistance and maintain it to 80% of T_{cr} until a rotation angle θ of about 0.02 rad/m. Under further loading, the specimens secured torsional resistance up to 50% of T_{cr} until 0.06 rad/m.

It is noteworthy that the design for torsion in EC 2 distinguishes the equilibrium torsion and the compatibility torsion according to the behavior of the structure. For the equilibrium torsion, where the torsional moment is required for the equilibrium of the structure, the reinforcement must secure a definite safety factor against the external loads. However, for the compatibility torsion, where the torsional moment results from the compatibility of deformations between members meeting at a joint [20], the minimum torsional reinforcement (Equation (1)) is employed to contribute to the redistribution of the load generated by the increase of the displacement [2]. For reference, in the ACI 318-14 code, the design torsion of the members for compatibility torsion is the cracking torsion given by the code [1], which means the reinforcement of the member is always greater than the minimum torsional reinforcement required by the code.

Considering EC 2, the results of Series 1 and 2 indicate that the member designed for the compatibility torsion with only $\rho_{v,min}$ of EC 2 could develop considerable torsional displacement enabling it to redistribute the load to the surrounding members even when the member experienced displacement-induced cracking. This means that $\rho_{v,min}$ applied in the design for the compatibility torsion of EC 2 cannot secure postcracking resistance comparable to that provided by the minimum reinforcement ratio applied in the design for shear or flexure but can reduce the possibility of the brittle behavior of the whole structure by redistributing the load.

Besides, in view of the results of Series 1, the reinforcement arranged with respect to the minimum torsional reinforcement ratio of ACI 318-14 and with additionally $\rho_{t+l} \geq 1\%$ is insufficient to prevent the loss of torsional resistance after cracking. However, Series 2 with lower ρ_{t+l} showed comparatively faster strength loss. This indicates that, under similar ρ_t, ρ_{t+l} influences the deformability.

The 18 specimens exhibited similar values for the torsional cracking moment T_{cr} since T_{cr} is more sensitive to the cross-sectional shape and tensile strength of concrete than to the amount of reinforcement. Table 5 arranges the values of T_{cr} for each specimen.

4.2.2. Transverse-to-Longitudinal Reinforcement Ratio ($\rho_t f_{yv}/\rho_l f_{yl}$) and Total Reinforcement Ratio (ρ_{t+l}). At the exception of specimen RA-SD4-3.5-0.5-2.13, ρ_{t+l} of Series 1 and 4 ranged between 1.62% and 1.63%. The comparison of their torsional behavior reveals that the specimens with larger ρ_t showed relatively more ductile behavior after cracking (Figures 6(a) and 6(d)). This means that, for similar ρ_{t+l}, the torsional ductility is secured with larger $\rho_t f_{yv}/\rho_l f_{yl}$. This tendency rejoins the conclusions of Chiu et al. [5]. For information, the choice of a low θ in the design results in smaller ρ_t, but the value of ρ_{t+l} remains practically unchanged because ρ_l must be increased to resist the required design torsional moment.

In view of the results of Series 3, 4, and 5 (Figures 6(c)–6(e)), the maximum torsional moment and the ductility increased when ρ_{t+l} increased for the same ρ_t. In other words, the increase of ρ_l lowered the angle of the concrete struts constituting the space truss, which improved the resistance to the torsional strength (T_n) by letting more stirrups resist to torsion.

4.2.3. High-Strength Reinforcement. In view of the results of Series 1 to 6, it was difficult to find a specific tendency in the relation between the use of high-strength reinforcement and the torsional behavior. Yoon et al. [7] pointed out that, in the case of stirrups with yield strength higher than 500 MPa, the risk of sudden loss of strength due to the crushing failure of the concrete struts is subjected to compression since the stirrups did not yield even under the maximum torsional moment (T_{max}). However, the torsion-rotation angle curves in Figure 6 did not show the expected sudden loss of the strength following the crushing failure of the concrete struts beyond T_{max}. Specifically, stable decrease of the strength seemed to occur. During the redistribution of the torsional load inside the member, the angle by which the concrete struts transferred the compressive force appeared to reduce and the load sustained by the reinforcement increased with larger displacement. Prior to the completion of the tests, the deformation of the specimens of Series 3 and 6 with the larger amount of high-strength reinforcement shown in Figure 7 also verified that crushing of the concrete struts did not happen beyond T_{max}.

4.3. Comparison of Predicted and Experimental Torsional Strengths. Table 5 compares the values of the torsional strengths T_{cr} and T_n predicted by Equations (2) and (3) derived from the thin-walled tube theory and the space truss analogy and those obtained experimentally. The predicted strengths vary according to the value of the effective thickness t assumed by the designer. Since t also interferes in the computation of A_0, its value affects both T_{cr} and T_n. In this study, the value of 85.7 mm is assumed for t based on the suggestion of EC 2 (EN 1992-1-1:2004 6.3.2 (1)). The experimental values of f_t and f_{yv} in Tables 2 and 3 are applied for each corresponding series.

The comparison reveals that the experimental values of T_{cr} and T_n are conservative reaching, respectively, 157% and 123% of the prediction on the average. The prediction appears to be more accurate for T_n than T_{cr}. Despite the assumption of t, the better prediction provided for T_n can be attributed to the comparatively even value of the yield strength of the reinforcement. On the contrary, the loss of accuracy in the prediction of T_{cr} can be explained by the reliance on the more versatile tensile strength of concrete, even if the effect of the subjective choice of the designer is reduced to some extent because A_0 decreases with larger t.

Table 5: Comparison of predicted and experimental torsional strengths.

Series	Designation of specimen	Prediction		Test		Test/prediction	
		T_{cr} (kN·m)	T_n (kN·m)	T_{cr} (kN·m)	T_n (kN·m)	T_{cr}	T_n
1	RA-SD4-1.3-0.3-1.62	40.4	38.8	67.2	55.6	1.66	1.43
	RA-SD5-1.5-0.2-1.62	40.4	47.2	68.4	57.9	1.69	1.23
	RA-SD6-1.5-0.2-1.62	40.4	52.0	63.1	60.0	1.56	1.15
2	RA-SD4-1.3-0.5-0.92	43.9	29.5	61.3	51.5	1.40	1.75
	RA-SD5-1.5-0.5-0.92	43.9	32.7	65.6	52.0	1.50	1.59
	RA-SD6-1.5-0.4-0.95	43.9	36.6	67.6	53.7	1.54	1.47
3	RA-SD4-3.2-0.3-3.28	36.9	89.6	63.2	86.8	1.71	0.97
	RA-SD5-3.2-0.3-3.21	36.9	94.6	65.2	88.0	1.76	0.93
	RA-SD6-3.2-0.2-3.21	36.9	108.0	63.6	89.4	1.72	0.83
4	RA-SD4-3.2-0.5-2.13	42.7	67.6	62.3	76.3	1.46	1.13
	RA-SD5-3.2-0.7-1.63	42.7	61.2	64.2	74.5	1.50	1.22
	RA-SD6-3.2-0.6-1.63	42.7	66.1	65.9	70.0	1.54	1.06
5	RA-SD4-3.2-1.1-1.33	45.0	46.5	74.2	70.0	1.65	1.51
	RA-SD5-3.2-1.0-1.26	45.0	48.6	67.7	65.5	1.50	1.35
	RA-SD6-3.2-0.8-1.26	45.0	54.0	66.1	69.9	1.47	1.29
6	RA-SD4-5.4-1.1-2.49	46.2	77.4	72.5	92.2	1.57	1.19
	RA-SD5-5.1-1.0-2.00	46.2	76.4	69.5	86.2	1.51	1.13
	RA-SD6-5.1-0.9-2.00	46.2	83.4	68.7	84.0	1.49	1.01
Average						1.57	1.23

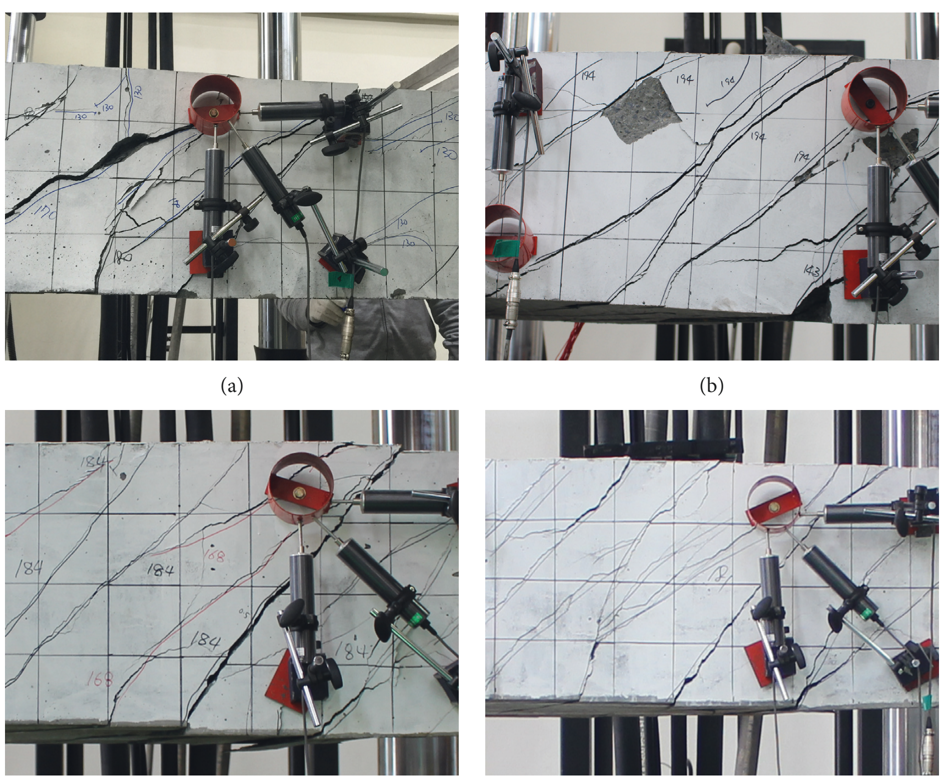

(a) (b) (c) (d)

Figure 7: Behavior of the softening zone in specimens using high-strength reinforcement. (a) Series 3: RA-SD5-3.2-0.3-3.21 ($\theta = 0.11$ rad/m, $T = 48.6$ kN·m). (b) Series 3: RA-SD6-3.2-0.2-3.21 ($\theta = 0.111$ rad/m, $T = 64.2$ kN·m). (c) Series 6: RA-SD5-5.1-1.0-2.00 ($\theta = 0.13$ rad/m, $T = 68.0$ kN·m). (d) Series 6: RA-SD6-5.1-0.9-2.00 ($\theta = 0.14$ rad/m, $T = 66.3$ kN·m).

5. Conclusions

This study evaluated the effect of the specifications recommended by current design codes (focused on Eurocode 2) for torsion on the torsional characteristics of 80 MPa high-strength concrete beams. To that goal, the torsion test was performed on beam specimens with rectangular cross section and various test variables involving the minimum torsional reinforcement ratio ($\rho_{v,min}$), the transverse-to-longitudinal reinforcement ratio ($\rho_t f_{yv}/\rho_l f_{yl}$), and the total reinforcement ratio (ρ_{t+l}). The following conclusions can be drawn:

(1) For the high-strength concrete beams, the adoption of $\rho_{v,min}$ recommended by EC 2 was insufficient to prevent the sudden loss of strength after the initiation of the torsional cracking.

(2) For the high-strength concrete beams, the application of $\rho_{v,min}$ and $\rho_{t+l} \geq 1\%$ recommended by ACI 318-14 was also insufficient to prevent the sudden loss of the torsional strength after cracking.

(3) With regard to the compatibility torsion of statically indeterminate structure (statically indeterminate torsion), the adoption of $\rho_{v,min}$ recommended by EC 2 secured enough deformability to allow the redistribution of the torsional moment.

(4) The ductile behavior could be secured with larger $\rho_t f_{yv}/\rho_l f_{yl}$ for the same ρ_{t+l}.

(5) The experimental results of this study did not reveal that the use of high-strength reinforcement with yield strength of 500 MPa has negative effect on the ductile behavior of the beam.

(6) The experimental data on the average gave conservative torsional cracking moment (T_{cr}) and torsional strength (T_n) reaching, respectively, 157% and 123% of the prediction from the formulae (Equations (2) and (3)) based on the thin-walled tube theory and space truss analogy with the effective thickness based on EC 2.

Data Availability

The data used to support the findings of this study may be available from the corresponding author upon request.

Additional Points

(i) The relation between the torsional cracking moment and the ductile behavior is discussed for the beam reinforced with the minimum torsional reinforcement ratio to examine the eventual properness of the minimum torsional reinforcement ratio recommended by Eurocode 2. (ii) The pure torsion test is performed on 18 beams made of 80 MPa concrete reinforced by high-strength bars with the rectangular section and various test variables involving the minimum torsional reinforcement ratio, the transverse-to-longitudinal reinforcement ratio, and the total reinforcement ratio. (iii) For the high-strength concrete beams, the minimum torsional reinforcement ratio recommended by Eurocode 2 is insufficient to prevent the sudden loss of strength after the initiation of the torsional cracking. (iv) But with regard to the compatibility torsion of statically indeterminate structure, the adoption of the minimum torsional reinforcement ratio recommended by Eurocode 2 may secure enough deformability under the displacement-controlled mode to allow the redistribution of the torsional moment.

Conflicts of Interest

The authors declare that there are no conflicts of interest regarding the publication of this paper.

Acknowledgments

This research was supported by a grant (13SCIPA02) from the Smart Civil Infrastructure Research Program funded by the Ministry of Land, Infrastructure and Transport (MOLIT) of the Korean government and Korea Agency for Infrastructure Technology Advancement (KAIA).

References

[1] ACI Committee, American Concrete Institute, and International Organization for Standardization, *Building Code Requirements for Structural Concrete (ACI 318-14) and Commentary (318R-14)*, American Concrete Institute, Farmington Hills, MI, USA, 2014.

[2] European Standards, *1-1: 2004 Eurocode 2: Design of Concrete Structures-Part 1-1: General Rules and Rules for Buildings*, European Standards, London, UK, 2004.

[3] L. J. Rasmussen and G. Baker, "Torsion in reinforced normal and high-strength concrete beams part 1: experimental test series," *Structural Journal*, vol. 92, no. 1, pp. 56–62, 1995.

[4] S. M. R. Lopes and L. F. A. Bernardo, "Cracking and failure mode in HSC hollow beams under torsion," *Construction and Building Materials*, vol. 51, pp. 163–178, 2014.

[5] H. J. Chiu, I. K. Fang, W. T. Young, and J. K. Shiau, "Behavior of reinforced concrete beams with minimum torsional reinforcement," *Engineering Structures*, vol. 29, no. 9, pp. 2193–2205, 2007.

[6] M. Ismail, *Behavior of UHPC Structural Members Subjected to Pure Torsion*, Vol. 24, Kassel University Press GmbH, Kassel, Germany, 2015.

[7] S. K. Yoon, S. C. Lee, D. H. Lee, and J. Y. Lee, "Failure modes of RC beams with high strength reinforcement," *Journal of the Korea Concrete Institute*, vol. 26, no. 2, pp. 143–150, 2014.

[8] K. N. Rahal and M. P. Collins, "Combined torsion and bending in reinforced and prestressed concrete beams," *ACI Structural Journal*, vol. 100, no. 2, pp. 157–165, 2003.

[9] K. N. Rahal and M. P. Collins, "Compatibility torsion in spandrel beams using modified compression field theory," *ACI Structural Journal*, vol. 103, no. 3, p. 328, 2006.

[10] C. E. Chalioris, "Behaviour model and experimental study for the torsion of reinforced concrete members," *WIT Transactions on the Built Environment*, vol. 85, 2006.

[11] L. F. A. Bernardo and S. M. R. Lopes, "Plastic analysis and twist capacity of high-strength concrete hollow beams under pure torsion," *Engineering Structures*, vol. 49, pp. 190–201, 2013.

[12] N. E. Koutchoukali and A. Belarbi, "Torsion of high-strength reinforced concrete beams and minimum reinforcement

requirement," *Structural Journal*, vol. 98, no. 4, pp. 462–469, 2001.

[13] ACI Committee, American Concrete Institute, and International Organization for Standardization, *Building Code Requirements for Structural Concrete (ACI 318-95) and Commentary (318R-95)*, American Concrete Institute, Farmington Hills, MI, USA, 1995.

[14] M. A. Ali and R. N. White, "Toward a rational approach for design of minimum torsion reinforcement," *ACI Structural Journal*, vol. 96, no. 1, pp. 40–45, 1999.

[15] K. Kim, D. Lee, M. K. Park, J. Y. Lee, and H. Ju, "Minimum torsional reinforcement ratio of reinforced concrete members for safe design," *Journal of the Korea Concrete Institute*, vol. 25, no. 6, pp. 641–648, 2013.

[16] I. K. Fang and J. K. Shiau, "Torsional behavior of normal-and high-strength concrete beams," *Structural Journal*, vol. 101, no. 3, pp. 304–313, 2004.

[17] K. N. Rahal, "Torsional strength of normal and high strength reinforced concrete beams," *Engineering Structures*, vol. 56, pp. 2206–2216, 2013.

[18] I. H. Yang, C. Joh, J. W. Lee, and B. S. Kim, "Torsional behavior of ultra-high performance concrete squared beams," *Engineering Structures*, vol. 56, pp. 372–383, 2013.

[19] M. M. Teixeira and L. F. A. Bernardo, "Ductility of RC beams under torsion," *Engineering Structures*, vol. 168, pp. 759–769, 2018.

[20] J. K. Wight and J. G. MacGregor, *Reinforced Concrete: Mechanics and Design 6E*, Pearson, London, UK, 2012.

[21] CSA, "Design of concrete structures," in *Standard CAN/CSA A23.3-04*, Canadian Standards Association, Mississauga, ON, Canada, 2004.

[22] FIB, *Model Code for Concrete Structures 2010*, Ernest and Son, Brigantine, NJ, USA, 2013.

[23] Korea Concrete Institute (KCI), *Structural Concrete Design Code*, Korea Concrete Institute (KCI), Seoul, South Korea, 2012.

[24] Korea Ministry of Land, Infrastructure and Transport (MOLIT), *Concrete Bridge Design Code, (Limit State Design)*, KDS, Issy-les-Moulineaux, France, 2016.

[25] C. E. Chalioris, "Experimental study of the torsion of reinforced concrete members," *Structural Engineering and Mechanics*, vol. 23, no. 6, pp. 713–737, 2006.


Journal of Engineering
The Scientific World Journal
International Journal of Rotating Machinery
Journal of Sensors
Advances in Multimedia
Advances in Civil Engineering
Journal of Control Science and Engineering
Journal of Robotics
Hindawi
Submit your manuscripts at
www.hindawi.com
Journal of Electrical and Computer Engineering
Advances in OptoElectronics
VLSI Design
International Journal of Navigation and Observation
Modelling & Simulation in Engineering
International Journal of Aerospace Engineering
International Journal of Chemical Engineering
International Journal of Antennas and Propagation
Active and Passive Electronic Components
Shock and Vibration
Advances in Acoustics and Vibration